Journal of Analytical and Applied Pyrolysis 118 (2016) 9–19

Contents lists available at ScienceDirect

Journal of Analytical and Applied Pyrolysis

journal homepage: www.elsevier.com/locate/jaap

Flame retardancy and thermal degradation behavior of efficient intumescent flame retardant LDPE composite containing 4A zeotile

Caimin Feng, Minyi Liang[1], Jiali Jiang, Jianguang Huang*, Hongbo Liu*

College of Applied Chemical Engineering, Shunde Polytechnic, Foshan 528333, China

ARTICLE INFO

Article history:
Received 23 October 2015
Received in revised form
29 November 2015
Accepted 6 December 2015
Available online 10 December 2015

Keywords:
Flame retardant mechanism
Thermal degradation behavior
4A zeotile
LDPE
Synergistic effect

ABSTRACT

The influence of 4A zeolite (4A) on the flame retardancy and thermal degradation behavior of efficient intumescent flame retardant low density polyethylene composites (LDPE/IFR) was investigated by the means of limited oxygen index (LOI), vertical burning test (UL-94), thermogravimetric analysis (TGA), thermogravimetric analyzer coupled to a mass spectrometer (TGA/MS), cone calorimeter test (CCT), digital photos, scanning electron microscopy (SEM), energy dispersive spectrometry (EDS) and laser raman spectroscopy (LRS). It was found that 4A dramatically enhanced the LOI value of the LDPE/IFR and all composites passed the UL-94 V-0 rating test. The TGA and TGA/MS results indicated that 4A apparently promoted to release more NH_3 at early stage, but reduced the main products intensity in the main degradation stage. Also, it enhanced the fire retardant performance with a great reduction in combustion parameters of LDPE/IFR composite from CCT test. The morphological structures observed by digital and SEM photos indicated that 4A promoted LDPE/IFR to form more compact and continuous char layer. The LRS and EDS analysis revealed that the compactness and strength of the char surface containing 4A was improved, and higher graphite degree was formed with remaining more P and O to increase the crosslinking degree.

1. Introduction

Polyethylene (PE) is widely used in many fields such as wire and cable, packing, pipes owing to its good flexibility at low temperatures, chemical stability, low toxicity, easy processing and excellent electric insulation properties [1].

Unfortunately, its low melting point and flammability limit its development in many applications. Therefore, it is necessary to improve both the fire retardancy and poor drip performance of PE [1]. One of simplest methods to improve the flame retardancy of PE is to add flame retardants. The most common fire retardants for PE are halogen based flame retardants, mineral fillers or intumescent flame retardants [1–3]. Halogen based flame retardants have excellent flame retardant performance, but they are now unacceptable for the environmental consideration. Mineral fillers, such as aluminum hydroxide and magnesium hydroxide, are environmental-friendly flame retardant additives for PE. However, high loadings are needed to meet the same flame retardant requirement in PE compared with halogen based retardants, allowing the mechanical properties of PE composites dramatically damage [3,4]. Therefore, to develop the halogen-free flame retardant PE with high flame retardant efficiency is very important.

Intumescent fire retardants (IFRs) are considered to be more promising candidates to replace halogen-based flame retardants for PE. The intumescent flame retardant systems are usually composed by charring agent, acid source and foaming agent. The ammonium polyphosphate (APP)/pentaerythritol (PER)/melamine (MEL) system is most common IFR system, and is widely used in polyolefin [3–11]. However, the conventional IFR presents some disadvantages, such as lower water resistance, lower flame retardant efficiency, ease to emigration, and lower thermal stability. Thus, it is essential to improve in the fire retardant efficiency and other properties of IFRs. Recently, triazine derivates are used as novel char-forming agents in IFRs with excellent charring ability, which are contributed to the presence of the tertiary nitrogen in the triazine rings [12–15].

In order to improve the flame retardancy of materials, many kind of synergistic agents have been used in IFR system to reinforce the flame retardancy, such as zeolites, organoboron siloxane, and some transitional metal oxides, metal chelates and metal compounds [16–21]. Previous researches have indicated that synergistic agents

* Corresponding authors. Fax: +86 75722328762.
E-mail addresses: hjguang@139.com (J. Huang), 962651061@qq.com (H. Liu).
[1] The author contributed equally to this work and should be considered co-first author.

http://dx.doi.org/10.1016/j.jaap.2015.12.008
0165-2370/

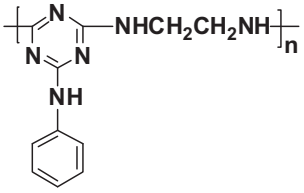

Scheme 1. Structure of CNCA-DA.

can effectively enhance the strength and stability of char layer and promote in catalyzing the reactions among IFR components.

In this work, an efficient charring agent (CNCA-DA) was designed and synthesized (see Scheme 1), which was an oligomeric triazine derivative. And it was expected to have good thermal stability, excellent water resistance and char-forming ability because of the presence of the triazine and benzene rigid rings [13]. 4A zeolite was chosen as a synergistic agent, who was cheap and have commercial significance. Its effects on the thermal degradation and flame retardancy of LDPE/IFR systems had been investigated by limiting oxygen index (LOI), vertical burning test (UL-94), thermogravimetry analysis (TGA), thermogravimetric analyzer coupled to a mass spectrometer (TGA/MS), cone calorimeter test (CCT), digital photographs, scanning electron microscopy (SEM), laser Raman spectroscopy (LRS) and energy dispersive spectrometry (EDS).

2. Experimental

2.1. Materials

4A zeotile with a diameter about 75 μm was offered by Shanghai Hengyu molecule sieve Co., Ltd., China. The Low Density Polyethylene (LDPE) resin (951-050, melt flow rate: 2–2.5 g/10 min) used in this work was offered by Maomin Petroleum Chemical Company, China. The charring agent (CNCA-DA) was synthesized in our laboratory and its structure is shown in Scheme 1 [13]. The Ammonium polyphosphate (APP) was produced by Shenzhen Anzheng Chemicals Company, China. The Antioxidant 1010 was produced by Ciba Specialty Chemicals, Switzerland.

2.2. Preparation

The flame retardant LDPE composites were prepared by melt blending at 110–120 °C by mixing pure LDPE, 4A zeotile with different content, APP, a charring agent (CNCA-DA) and some amount of antioxidant and 4A in the two-roll mill with a rotor speed of 60 rpm, and the mixing time was 8 min for each sample. Then the composites were pressed on a curing machine for 2 min to produce various thick sheets, which were used to produce various dimension sheets for LOI and UL-94 tests.

2.3. Flame retardancy test

The LOI data of all the composites were got at room temperature on an oxygen index instrument (DRK304B) produced by Jinan Deruike Instrument Factory according to ASTM D 2863-97 standard. The dimensions of all the samples were $130 \times 10 \times 4\,mm^3$. The vertical burning rates (UL-94) of all samples were measured on a CZF-3 instrument produced by Jiangning Analysis Instrument Factory, with the sample dimensions of $125 \times 12.5 \times 3.2\,mm^3$. The UL-94 test results were classified by burning ratings V-0, V-1 or V-2. V-0 rating demonstrated composites with the best flame retardancy.

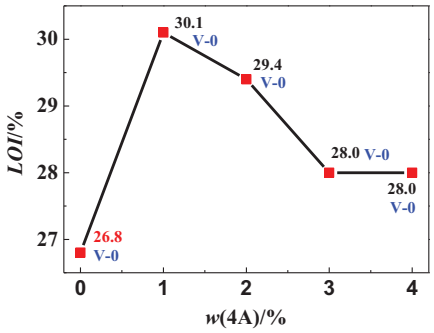

Fig. 1. Effect of 4A addition on the flame retardant properties of LDPE/IFR composites.

2.4. Thermogravimetric analysis (TGA)

The thermal gravimetric analysis (TGA) was performed on thermogravimetric analyzer (TA Q500, USA) at a heating rate of 10 °C/min ranging from room temperature to 800 °C. The about 5 mg sample was examined under air flowing rate of 40 ml/min. All the thermal degradation data were obtained from TG and DTG curves directly.

2.5. Cone calorimeter test (CCT)

All the CONE data were obtained from the Cone Calorimeter (manufactured by Fire Testing Technology) at a heat flux of $35\,kW\,m^{-2}$ according to ISO 5660-1 standard. All the samples ($100 \times 100 \times 4\,mm^3$) were laid on a horizontal sample holder.

2.6. Thermogravimetric analyzer coupled to a mass spectrometer (TGA/MS)

TGA/MS characterization was performed on a Thermo Mass photo instrument. TGA was performed in argon of high purity at a flow rate of 20 ml/min. In the experiment, all samples weighing about 10 mg were tested with heating rate of 20 °C/min from room temperature to 800 °C.

2.7. Laser Raman spectroscopy analysis

The Laser Raman spectroscopy (LRS) measurements were carried out by Raman microspectrometer (Renishaw inVia) at room temperature with excitation by a 514.5 nm helium–neon laser line, and the scanning range was within the 50–4000 cm^{-1} region. To avoid sample heating, the power was kept below 4 mW.

2.8. Scanning electron microscopy-energy dispersive X-ray spectrometry (SEM-EDS)

The scanning electron microscopy (SEM) was performed by using a SU8010 SEM (Hitachi, JPN) to observe the morphology of the char residue, whose accelerating voltage was 10 kV. The surface of the char residues wasn't sputter-coated before examination. All the chars for SEM were treated in muffle at 500 °C for 5 min.

Energy dispersive X-ray spectrometry (EDS) analysis data of the char were measured by an energy dispersive X-ray spectrometer (Horriba EMAX) without sputter-coating.

Table 1
Catalytic effects of 4A.

4A%	LOI/%	△LOI/%	4A/wt%	CAT-EFF[a]
0	26.8	–	–	–
1	30.1	3.3	1	3.3
2	29.4	2.6	2	1.3
3	28.0	1.2	3	0.4
4	28.0	1.2	4	0.3

[b] 4A/wt% means 4A concentration in LDDPE/IFR/4A.
[a] CAT-EFF = $\triangle LOI/wt_{4A}\%$. . . . . .(1).

3. Results and discussion

3.1. Effect of 4A on the flame retardancy of LDPE/IFR composites

Fig. 1 presents the LOI value and UL rating of LDPE/IFR composites varies with different 4A content at the IFR amount of 25 wt%. The LOI value of LDPE/IFR composite is 26.8% and it reached UL-94 V-0 rating. The LOI values of composites firstly increased rapidly with increasing the content of 4A in the LDPE/IFR composites. When the content of 4A increased to 1.0 wt%, the LOI value reached the maximum value of 30.1%. However, the LOI values began to decrease slightly with further loading of 4A. When the content of 4A was 4 wt%, the LOI value decreased to 28.0%, but it was still higher than that of LDPE/IFR composite and passed UL-94 V-0 rating. The LOI and UL-94 tests results suggested that there was an optimum content of 4A, where an obvious synergistic effect exited between 4A and the IFR, and the higher loading of 4A destroyed the balance between the swelling behavior and carbonization function of the LDPE/IFR systems and decreased the LOI value [22–24].

3.2. Catalytic effectivity analysis

The catalytic effectivity (CAT-EFF) for catalysts is defined as the increment in LOI per mass percent of catalysts at the optimal concentration of the catalyst [16,17] as shown in formulation (1). Table 1 listed the CAT-EFF of 4A for LDPE/IFR systems. It could be seen from Table 1 that as the increasing loading of 4A, the CAT-EFF of LDPE/IFR composites gradually decreased. When the loading of 4A was 1%, the LDPE/IFR composite had the highest LOI value (30.1%) and the highest CAT-EFF value (3.3), which indicated that 1% 4A was most effective for the LDPE/IFR composites with 25 wt% IFR loading.

$$\text{CAT-EFF} = \triangle LOI/wt(4A)\% \quad (1)$$

3.3. Thermal degradation behaviors of IFR and LDPE composites

The mass ratio of IFR/4A was 20:1. The TGA and DTG curves of IFR and IFR/4A systems were analyzed by TGA under air atmosphere, and the curves are presented in Fig. 2, and the analysis results are summarized in Table 2. The IFR had good thermal stability, and its initial decomposing temperature was 313 °C, based on the 5% mass loss ($T_{5\%}$). According to DTG curves, thermal degradation behavior of IFR was divided into three steps (Fig. 2(b)). The peak of step one occurred at 309 °C, which was assigned to the releases the water, ammonia; and the second one at 374 °C was assigned to the char-forming and decomposition of IFR; the third one happened at 596 °C, which could be attributed to the degradation of char residue [12].

4A lowered the initial degradation temperature ($T_{5\%}$) of IFR system from 313 to 293 °C (Fig. 2 and Table 2). The DTG curve of IFR/4A system showed that its thermal degradation behavior was similar to that of IFR, and it was also classified in three steps. The first peak at 309 °C related to the release of water and ammonia, but more degradation product was formed; and the second one at 385 °C related to the decomposition and char-forming of IFR/4A, and its value is higher than that of IFR system. The last peak appeared at 605 °C, whose value is higher than that of IFR system at the same peak, and it was contributed to the decomposition of char residue.

Table 2
TGA data of IFR under air.

	IFR[a]	IFR/4A[b]	IFR/4A calculation[c]
[d] $T_{5\%}$/°C	313	293	351
[d] $T_{10\%}$/°C	349	324	378
[d] $T_{50\%}$/°C	569	585	470
[e] T_p/°C	374	386	374
[f] $W_{600\,°C}$/%	41.0	48.5	12.2
[f] $W_{700\,°C}$/%	18.2	41.6	5.5
[f] $W_{800\,°C}$/%	8.7	35.8	4.3

[a] IFR is composed by APP and CNCA-DA, and the mass ratio of APP:CNCA-DA is 2:1.
[b] The mass ratio of IFR:4A is 20:1.
[c] $W_{calculation} = W_{IFR} \times 95.2\% + W_{4A} \times 4.8\%$...(1).
[d] $T_{5\%}$, $T_{10\%}$ and $T_{50\%}$ are the temperature at which 5%, 10% and 50% weight loss occurs, respectively.
[e] T_p is the temperature at which the maximum of weight loss rate take place.
[f] $W_{600\,°C}$/%, $W_{700\,°C}$/% and $W_{800\,°C}$/% are the residue of materials at 600, 700 and 800 °C.

Table 3
TGA data of LDPE and LDPE composites under air atmosphere.

	LDPE	LDPE/IFR[a]	LDPE/IFR/1%4A[b]	LDPE/IFR/1%4A calculation[c]
[d] $T_{5\%}$/°C	328	355	347	351
[d] $T_{10\%}$/°C	351	373	383	378
[d] $T_{50\%}$/°C	391	470	473	471
[e] T_p/°C	390	488	485	485
[f] $W_{600\,°C}$/%	0.6	11.3	14.6	12.2
[f] $W_{700\,°C}$/%	0.6	2.5	8.1	5.5
[f] $W_{800\,°C}$/%	0.5	1.4	5.8	4.3

[a] IFR is composed by APP and CNCA-DA, and the mass ratio of APP:CNCA-DA is 2:1, and the IFR content is 25 wt%.
[b] The 4A content is 1 wt% in LDPE/IFR/1%4A composite.
[c] $W_{calculation} = W_{LDPE/IFR} \times 99\% + W_{4A} \times 1\%$. . .(2).
[d] $T_{5\%}$, $T_{10\%}$ and $T_{50\%}$ are the temperature at which 5%, 10% and 50% weight loss occurs, respectively.
[e] T_p is the temperature at which the maximum of weight loss rate take place.
[f] $W_{600\,°C}$/%, $W_{700\,°C}$/% and $W_{800\,°C}$/% are the residue of materials at 600, 700 and 800 °C.

Curve of IFR/4A was the experimental result of IFR/4A system, and curve of IFR/4A (calculation) was the result calculated from curves of IFR and 4A based on their percentage in IFR/4A system according formula (2). Comparing to these TGA and DTG curves of IFR/4A and IFR/4A (calculation), the thermal degradation behavior of IFR/4A presented great difference, especially in the range of high temperature. The second and third peaks on IFR/4A system decreased compared with IFR and IFR/4A (calculation), especially the third peak. The char residue of IFR/4A was 48.5%, 41.6% and 35.8 % at 600, 700 and 800 °C, respectively, which were far higher than those of IFR and IFR/4A (calculation). These facts suggested that by incorporation of 4A into IFR, the thermal degradation behavior of IFR changed, and 4A enhanced the char-forming ability and thermal stability of IFR, and the interaction between 4A and IFR leaded to the formation of some new substances which are more stable at high temperature [12,24].

$$w_{calculation} = w_{IFR} \times 95.2\% + w_{4A} \times 4.8\% \quad (2)$$

Fig. 3 shows the TGA (a) and DTG (b) curves of LDPE and LDPE composites, and the results are listed in Table 3. There was only one sharp peak in the DTG curve of LDPE, and the peak appeared at 390 °C with only 0.6% residue at 600 °C. LDPE/IFR and LDPE/IFR/1%4A systems had similar TGA and DTG curves, but they have lower weight loss rate and higher thermal stability comparing with pure LDPE. The existence of 4A decreased the initial degrada-

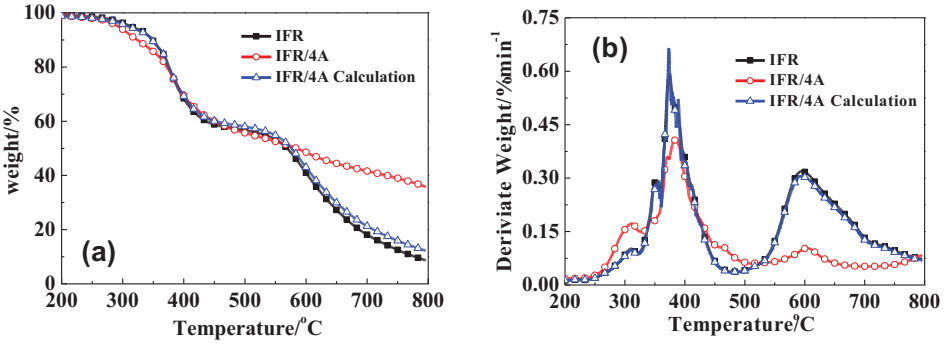

Fig. 2. TGA (a) and DTG (b) curves of flame retardants with or without 4A under air atmosphere.

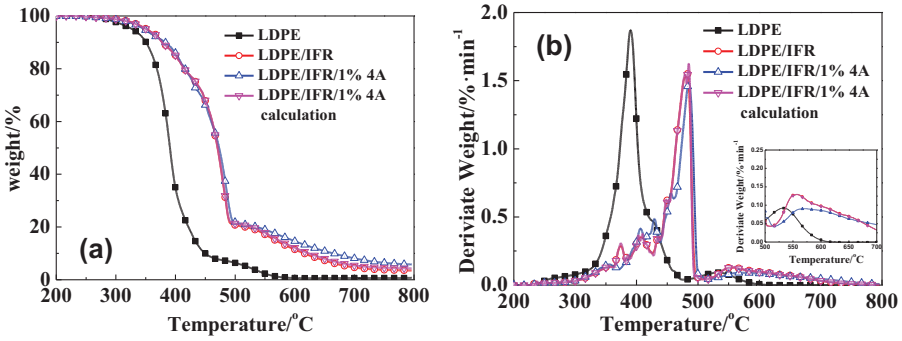

Fig. 3. TGA (a) and DTG (b) curves of LDPE and its composites under air atmosphere.

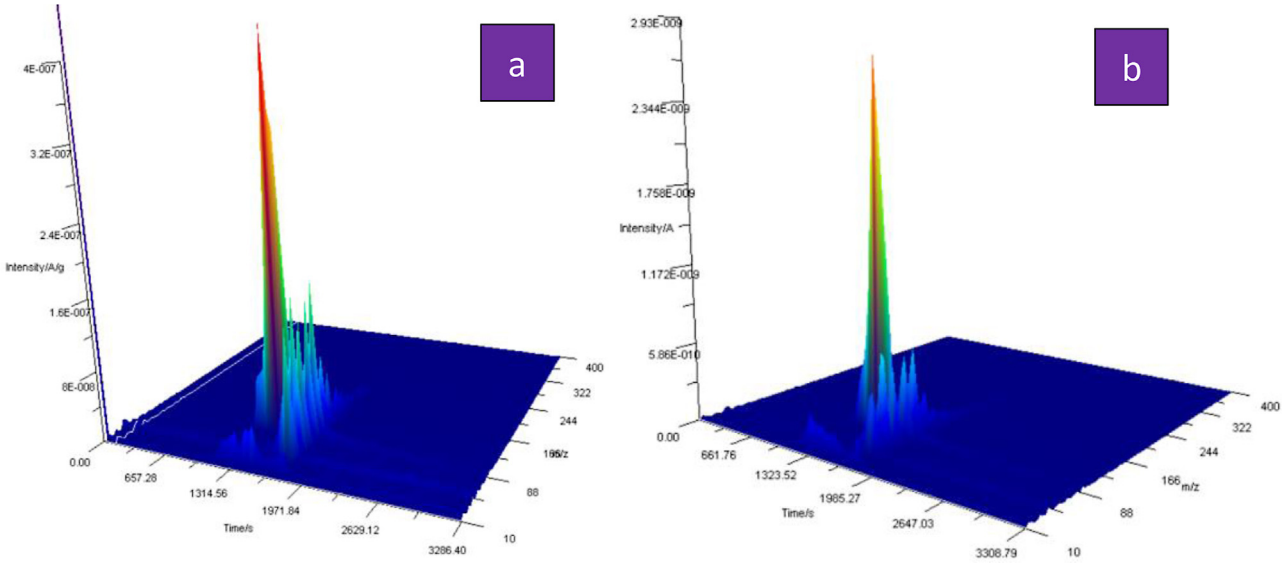

Fig. 4. 3D TGA-MS spectra of LDPE/IFR (a) and LDPE/IFR/1%4A (b).

tion temperature ($T_{5\%}$) from 355 to 347 °C, but it had higher $T_{10\%}$ and $T_{50\%}$, which demonstrated that 4A promoted IFR to degrade at advance, and the char layer was more stable than that of LDPE/IFR composite.

Curve of LDPE/IFR/1%4A (calculation) was the result calculated from curves of LDPE/IFR and 4A based on their percentage in LDPE/IFR/1%4A system according formula (3). On Comparison to LDPE/IFR/1%4A (calculation), the LDPE/IFR/1%4A composite presented higher thermal stability at high temperature. The char residues of LDPE/IFR/1%4A composite at 600, 700 and 800 °C were 14.6%, 8.1% and 5.8% respectively, which were much higher than those of LDP/IFR and LDP/IFR/4A (calculation). These results indicated that the present of 4A improved char formation ability of the LDPE/IFR composite at high temperature.

$$W_{\text{calculation}} = W_{\text{LDPE/IFR}} \times 99\% + W_{4A} \times 1\% \quad (3)$$

TGA/MS was employed to characterize the main volatile products derived from the pyrolysis of the LDPE/IFR and LDPE/IFR/1%4A composites, and the database of the National Institute of Standards and Technology (NIST) [25] was occupied to determinate the atomic mass units. Figs. 4 and 5 present the 3D TGA-MS spectra and Main ion current curves for species produced from degradation of LDPE/IFR and LDPE/IFR/1%4A composites. In case of the two com-

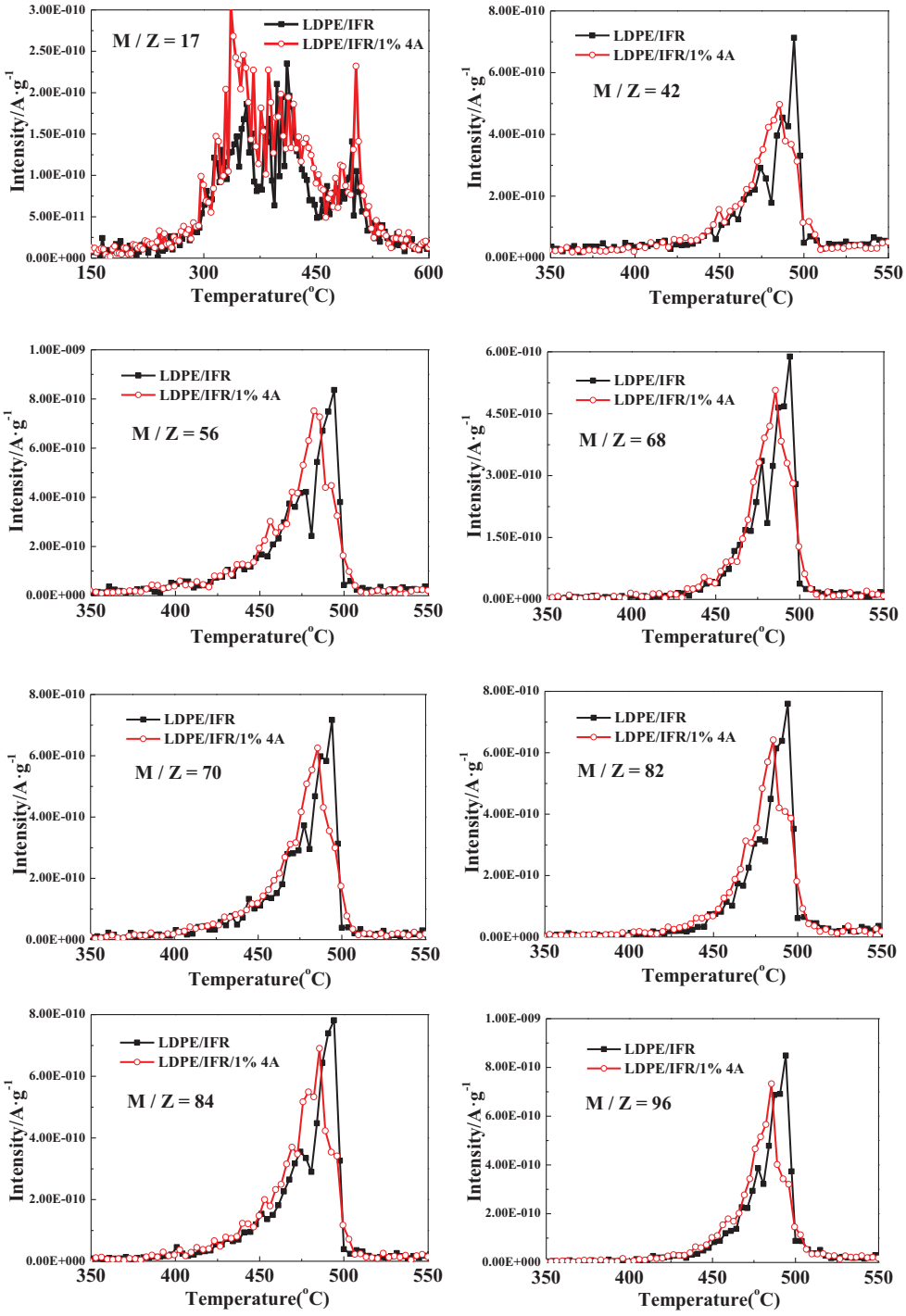

Fig. 5. Main ion current curves for species produced from degradation of LDPE/IFR and LDPE/IFR/1%4A.

posites, the main ion current peaks were at m/z 17, 42, 56, 68, 70, 82, 84, 96, 98, 108, 110 and 112, and they were different significantly.

The ion current peaks at $m/z = 17$ was assigned to NH_3. The two samples released NH_3 at the range from 250 to 550 °C, and the peak intensity of LDPE/IFR/1%4A sample was higher than that of LDPE/IFR, which indicated that 4A promoted IFR to degrade more NH_3, and increased releasing rate of NH_3, which agreed with the results of TGA.

In case of the ion current peaks at $m/z = 42$, 56, 68, 70, 82, 84, 96, 98, 108, 110 and 112, their intensity of LDPE/IFR/1%4A sample were lower than those of LDPE/IFR sample. The peak at $m/z = 42$ was assigned to be ketene; and the peak at $m/z = 56$ was attributed to C-4 compound, for example butylene; and the peaks at $m/z = 68$, 70 were attributed to C-5 compounds, such as pentene, pentadiene, or pentyne; and the peak at $m/z = 82$, 84 was considered to be C-6 compounds, such as cyclohexene, butylethene, or hexadiene; and the peaks at $m/z = 96$, 98 were contributed to C-7 or C-6 compounds, such as heptylene, heptadiene, or hexanone; and the peaks at $m/z = 108$, 110 and 112 were assigned to octane, octadiene [26]. These results demonstrated that 4A increased releasing rate of NH_3, but decreased others products of thermal degradation, and chain

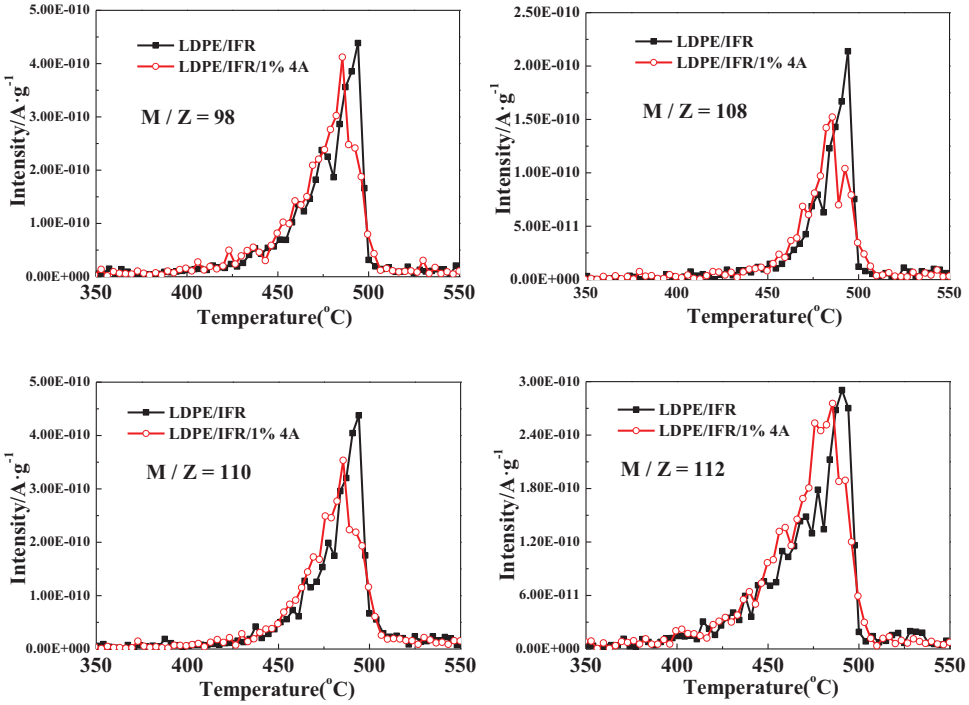

Fig. 5. (*Continued*).

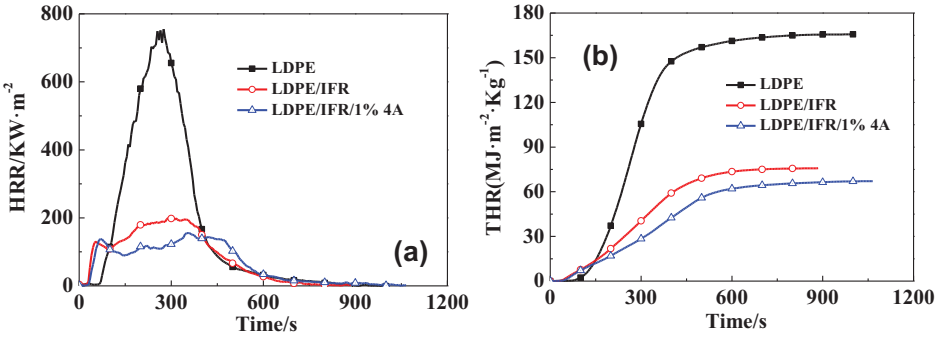

Fig. 6. The HRR (a) and THR (b) curves of LDPE and LDPE composites.

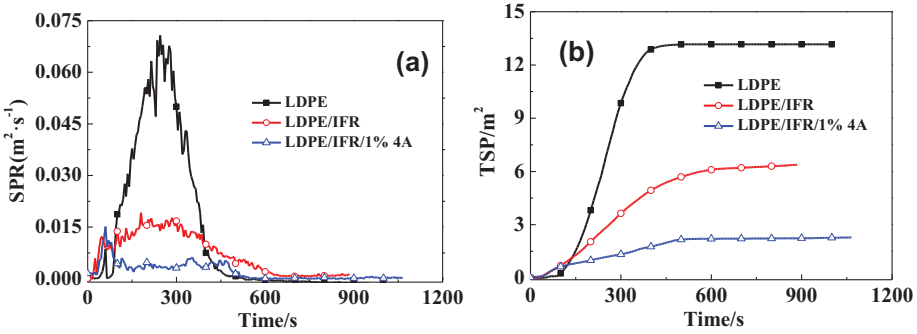

Fig. 7. The SPR (a) and TSP (b) curves of LDPE and LDPE composites.

fragmentation was the main mechanism of thermal degradation in the thermal decomposition step.

3.4. Fire properties of the LDPE and its flame retardant composites

Cone calorimetric (CCT) analysis is occupied to characterize the flame retardant parameters of flame retardant materials frequently, which has good correlation with real fire disaster. So it is often employed to forecast the flame behavior of flame retardant materials in real fires [22–25]. The principal fire properties including the heat release rate (HRR), the peak heat release rate (PHRR), the total heat release (THR), mass loss (ML), and CO production rate (COP), CO_2 production rate (CO_2P) are determined by CCT. Figs. 6–9 and Table 3 show the plots and the detailed informa-

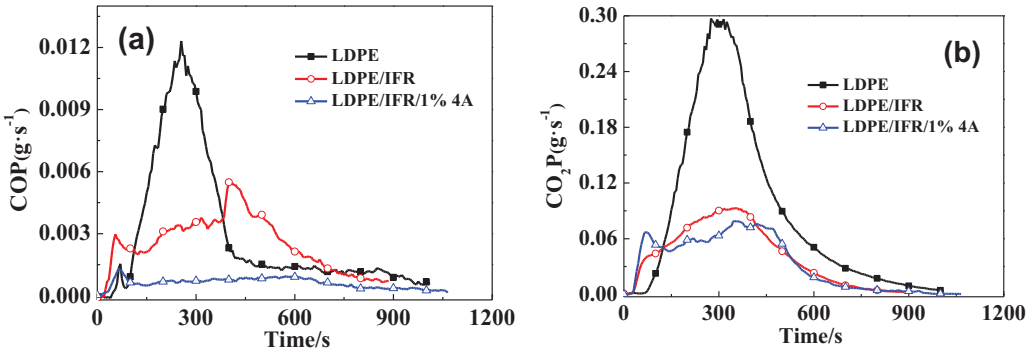

Fig. 8. The COP (a) and CO2P (b) curves of LDPE and LDPE composites.

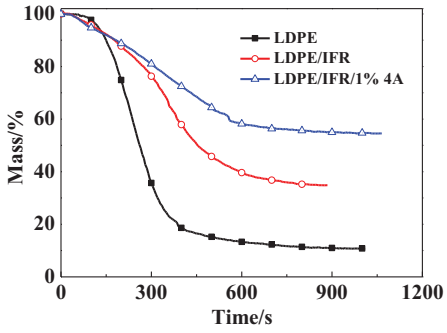

Fig. 9. The Residual Mass curves of LDPE and LDPE composites.

tion of combustion behavior for LDPE, LDPE/IFR and LDPE/IFR/1%4A (with 1%wt 4A) obtained from the cone calorimeter test at a heat flux of 35 kW m^{-2}.

The HRR and THR are considered to be the most critical parameters to estimate the intensity of fires, and the excellent flame retardant system presents low HRR and THR value. Fig. 6(a and b) shows the HRR and THR curves of LDPE, LDPEP/IFR and LDPEP/IFR/4A composites. It was found that pure LDPE burned very fast after ignition with a sharp HRR peak, and p-HRR and THR value were 755 kW m^{-2} and i 165 MJ m^{-2} kg respectively. In case of LDPE/IFR and LDPE/IFR/1%4A composites, their p-HRR values reduced remarkably from 755 kW m^{-2} to 200 and 155 kW m^{-2} respectively, and the decrease in peak of HRR is nearly 73.5% and 79.5%. Moreover, the combustion time of the LDPE/IFR and LDPE/IFR/1%4A composites was prolonged in comparison with that of pure LDPE. The HRR curve of LDPE/IFR and LDPE/IFR/1%4A composites showed two peaks, but the peaks of LDPE/IFR/1%4A composite appeared later with lower HRR values than those of LDPE/IFR composite. As shown in Fig. 6(b), it was obvious that LDPE/IFR and LDPE/IFR/1%4A showed a much lower THR, and these values decreased significantly from 165 MJ m^{-2} kg for pure PP to 76

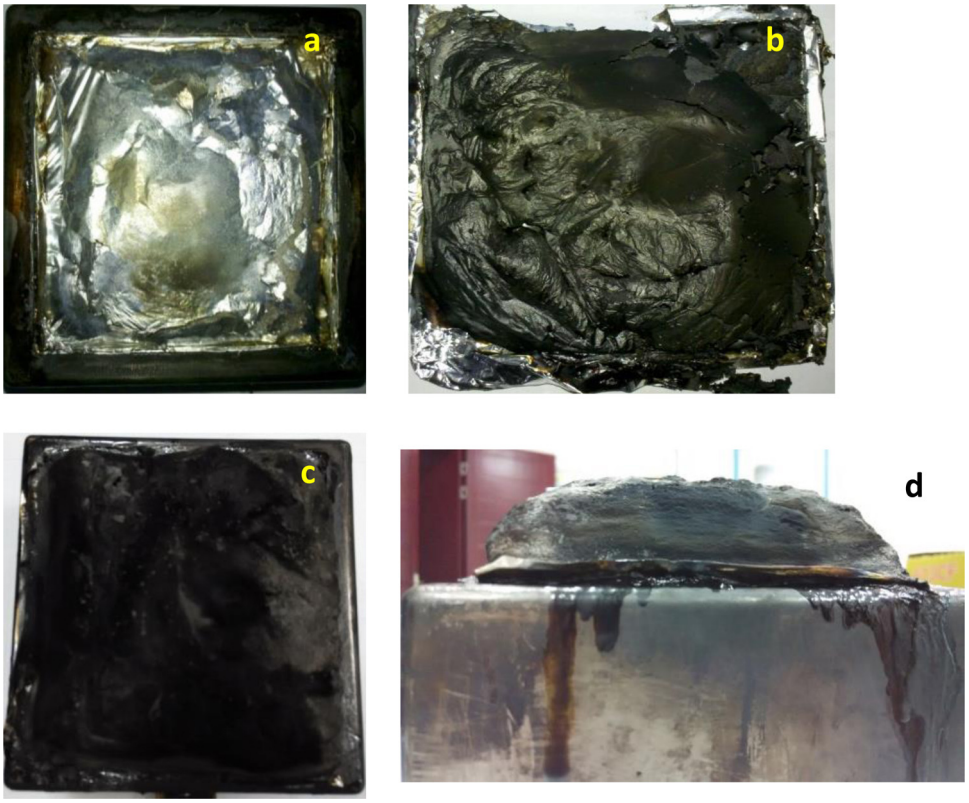

Fig. 10. Photographs of the samples after cone calorimeter test (a) LDPE, (b) LDPE/IFR, (c) LDPE/IFR/1%4A and (d) LDPE/IFR/1%4A.

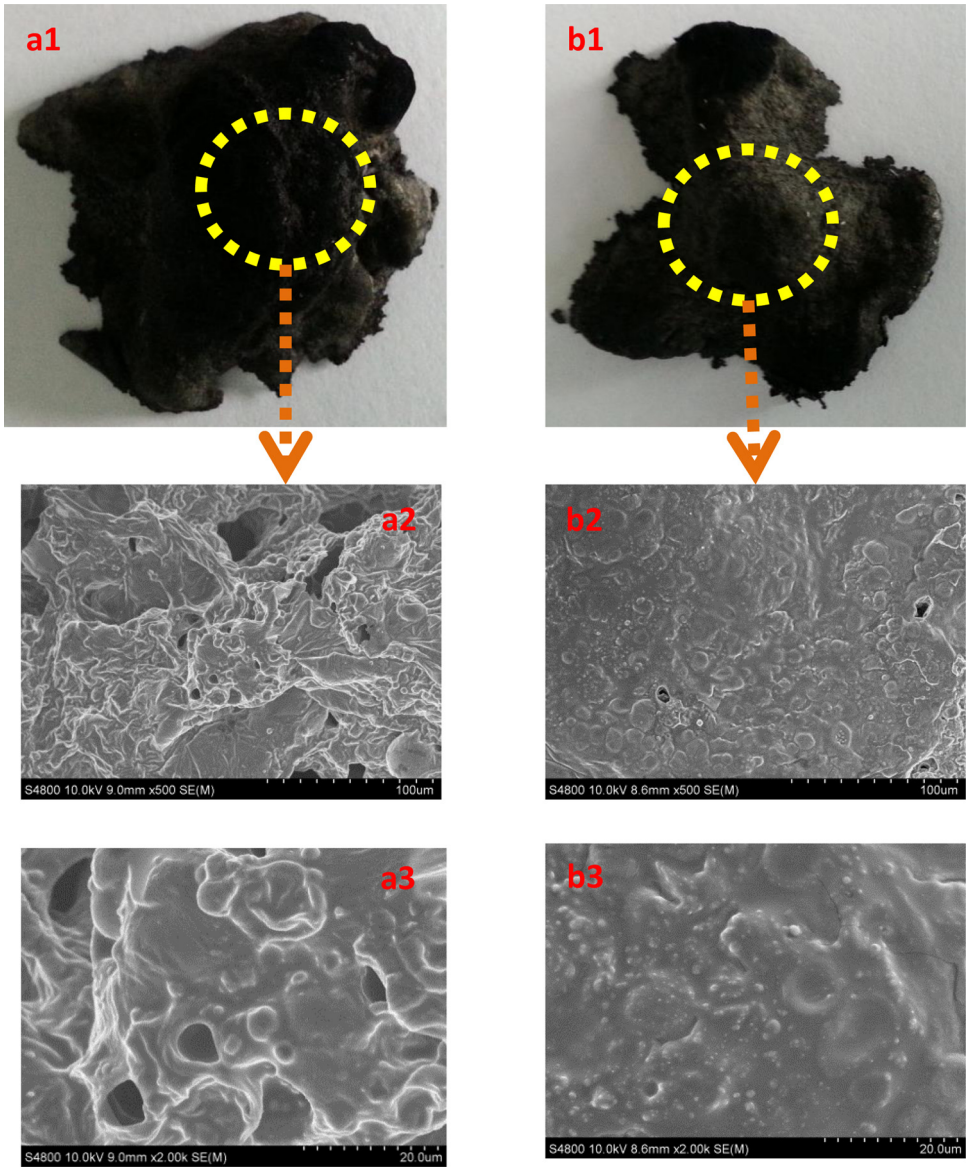

Fig. 11. SEM micrographs of char residue of char residue LDPE/IFR (a) LDPE/IFR/1%4A (b) after heated in muffle furnace at 500 °C Zoom: a2, b2 × 500, a3, b3 × 2000.

and 36 MJ m^{-2} kg respectively. This was contributed to the incorporation of 4A into LDPE/IFR composite, 4A promoted the strength and compactness of intumescent char layer, which restricted heat from cone calorimeter and hindered material pursuing the further combustion.

Fig. 7(a and b) presents the SPR and TSP curves of LDPE, LDPE/IFR and LDPE/IFR/1%4A composites. The smoke emission also plays a critical role in fire hazard including smoke production rate (SPR) and total smoke production (TSP). The SPR curves of the LDPE/IFR and LDPE/IFR/1%4A were much lower than that of LDPE, similar to HRR curves, and the peak SPR value decreased from 0.07 to 0.02 and 0.015 m^2 s^{-1} at first peak. Meanwhile, TSP curves showed the similar trend as TSP curves, and TSP value decreased from 13.1 m^2 of LDPE to 6.4 and 2.2 m^2 for LDPE/IFR and LDPE/IFR/1%4A, respectively. The results indicated that the SPR and TSP of LDPE/IFR/1%4A was much lower than those of LDPE and LDPE/IFR, and the reason was that the synergistic effect of 4A to promote IFR to form more stable char layer, and the formed char layer served as better thermal insulator to prevent the smoke production and emission.

Fig. 8(a and b) presents the COP and CO_2P curves of LDPE, LDPE/IFR and LDPEA/IFR/4A composites. The COP curves of LDPE/IFR and LDPE/IFR/1%4A composites presented two peaks, but only one sharp peak appeared in LDPE. The COP curve for LDPE/IFR and LDPE/IFR/1%4A composites were much lower than that of LDPE, and especially the peak values of LDPE/IFR/1%4A composite were far lower than those of LDPE and LDPE/IFR. The CO_2P curves in Fig. 8(b) are similar to the HRR curves, and the LDPE/IFR/1%4A composites also had two peaks. The peak values of CO_2P for LDPE/IFR/1%4A composite was 0.067 and 0.079 g s^{-1} respectively, and they were lower than those of pure LDPE and LDPE/IFR. These results also indicated that 4A promoted to form more compact char layer to suppress the generation of CO and CO_2.

Fig. 9 presents the dynamic curves of mass varying time for LDPE, LDPE/IFR and LDPE/IFR/1%4A composites. LDPE/IFR/1%4A composite lost its mass more slowly than those of LDPE and LDPE/IFR composite. At 400 s, the residual mass of LDPE, LDPE/IFR and LDPE/IFR/1%4A composites were 18.6 %, 57.9 % and 72.5 % respectively. These results revealed that the compact char layer decreased the evolution of combustible gas during the combustion process, and 4A helped form more compact char layer.

Fig. 10 shows the digital photographs of the residues of LDPE, LDPE/IFR and LDPE/IFR/1%4A composites after cone calorimeter

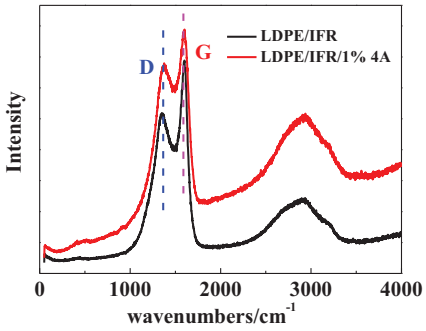

Fig. 12. Raman spectra of char residues of LDPE composites.

tests. The pure LDPE left almost nothing after burned, while thick and intumescent char layers were formed in the case of LDPE/IFR and LDPE/IFR/1%4A, which served as physical shield and prevented heat and combustible gas from transferring between the flame zone and the burning substrate. Also, the char formed by LDPE/IFR/1%4A composite was higher than that of LDPE/IFR, and more compact and continuous char was formed, which improved the shield ability of char layer.

3.5. Morphology of the final char

The microstructure of intumescing char plays a critical role in flame retardant properties of polymeric materials. In order to investigate the synergistic effect of 4A on the flame retardant mechanism, the intumescing char residue of LDPE/IFR and LDPE/IFR/1%4A was observed by SEM and magnified by 500 and 2000 times, as shown in Fig. 11. Both samples (with and without 4A) produced a continuous, compact and intumescent char layer, which could act as an insulating shield to prevent the oxygen and heat from permeating to reach the underlying material. It showed that the char surface for LDPE/IFR/1%4A (Fig. 11b2 and b3) was more homogenous and compact than that of LDPE/IFR (Fig. 11a2 and a3). Relative to LDPE/IFR system, the char surface of LDPE/IFR/1%4A is more compact with less bubbles appearing on their surfaces, which indicated that 4A promoted to form more compact char layer with better mechanical performance, consequently the reinforced char layer with some crosslink network possessed higher thermal stability [22–24]. Therefore, during burning, heat and flammable volatiles could hardly penetrate the char layer into the flame zone for LDPE/IFR/1%4A.

3.6. Chemical composition of the final char

Raman spectrum is usually used to characterize graphitic structure of materials, and to evaluate the order degree of carbon materials in terms of two characteristic bands: G band (about 1600 cm^{-1}, showing the graphitic structure, corresponded to an E2 g mode of hexagonal graphite, relating to the vibration of sp2-bonds carbon atoms in graphite layers) and D band (about 1360 cm^{-1}, representing the unorganized carbon structure, associated with vibration of carbon atoms with dangling bonds in the plane terminations of disordered graphite or glass carbons) [16,17,24].

The Raman spectra of the char residue for LDPE/IFR and LDPE/IFR/1%4A composites after treated at 500 °C for 5 min are presented in Fig. 12, and all of them exhibited two visible bands (D and G band), and these observations provided a positive evidence for the formation of polyaromatic species or graphitic structures. Each curve was subjected to peak fitting by using the curve fitting software Origin 8.5/Peak Fitting Module to divide the curve into 2 Gaussian bands [27,28] (Table 4).

Table 4
Cone results of flame retardant materials.

Properties	LDPE	LDPE/IFR	LDPE/IFR/1%4A
Peak1-HRR/KW m^{-2}	755	131	137
$t_{peak1\text{-}HRR}$/s	275	55	175
Peak2-HRR/KW m^{-2}	–	200	155
$t_{peak2\text{-}HRR}$/s	–	290	460
THR/MJ m^{-2} kg	165	76	36
Peak1-SPR/m^2 s^{-1}	0.007	0.001	0.015
$t_{peak1\text{-}SPR}$/s	60	50	165
Peak2-SPR/m^2 s^{-1}	0.07	0.02	0.006
$t_{peak2\text{-}SPR}$/s	245	180	460
TSP	13.1	6.4	2.2
Peak1-COP/m^2 s^{-1}	0.0015	00030	0.0013
$t_{peak1\text{-}COP}$/s	70	55	170
Peak2-COP/m^2 s^{-1}	0.012	0.0055	–
$t_{peak2\text{-}COP}$/s	255	400	–
Peak1-CO_2P/m^2 s^{-1}	0.30	0.093	0.067
$t_{peak1\text{-}CO2P}$/s	275	355	175
Peak2-CO_2P/m^2 s^{-1}	–	–	0.079
$t_{peak2\text{-}CO2P}$/s	–	–	455
Char residue at 400 s/%	18.6	57.9	81.6

Peak1-HRR and Peak2-HRR: the first and second peak value on the heat release rate (HRR) curves; $t_{peak1\text{-}HRR}$ and $t_{peak2\text{-}HRR}$: time to first and second peak heat release; THR: total heat release; Peak1-SPR, and Peak2-SPR: the first and second peak value on the smoke production rate (SPR) curves; $t_{peak1\text{-}SPR}$, and $t_{peak2\text{-}SPR}$: time to first and second peaks of smoke production rate; TSP: total smoke produce; Peak1-COP and Peak2-COP: the first and second peak value on the CO production rate (COP) curves; $t_{peak1\text{-}COP}$ and $t_{peak2\text{-}COP}$: time to first and second peaks of CO production rate curves; Peak1-CO_2P: the first peak value on the CO_2 production rate (CO_2P) curves; $t_{peak1\text{-}CO2P}$ and $t_{peak2\text{-}CO2P}$: time to first and second peaks of CO_2 production rate curves; Char residue at 400 s: mass percentage left when testing at 400 s.

The relative intensity (area) ratio R of the D band to the G band is inversely proportional to an in-plane microcrystalline size and/or an in-plane phonon correlation length [28]. Therefore, the R value is a good guide for the graphitization degree of carbon materials, the lower the value of R, the higher the graphitization degree of chars. Table 5 shows the results of Raman analysis of the char for LDPE/IFR and LDPE/IFR/1%4A systems. The R values of chars for LDPE/IFR and LDPE/IFR/1%4A were 2.18 and 1.94 respectively, which indicated graphitic structure changed obviously during burning owing to the presence of 4A. Combined with the SEM and LRS results, it was concluded that when the composite was ignited, 4A turned amorphous char into graphitic structure on the surface that enhanced the flame retardant properties.

In order to investigate the relationship between the chemical component of char and the flame retardant properties, the energy dispersive spectrometry (EDS) was employed to characterize the component of final char residue. Fig. 13 give the EDS spectra of the char residue for LDPE/IFR and LDPE/IFR/1%4A composites after treated at 500 °C for 5 min, and the results are listed in Table 6. When 1% 4A was incorporated into LDPE/IFR composite, the O content on the char surface was a little higher than that of LDPE/IFR, and the relative contents of P and O for LDPE/IFR/1%4A composite were also higher than those of LDPE/IFR composite. The results suggested that the existence of 4A was helpful to form more connected structures containing O and P elements and improve the strength of char layer to flame retardant properties [16].

Table 5
Results of Raman analysis of char residues for LDPE/IFR and LDPE/IFR/1%4A.

Sample	A_D	A_G	$R = A_D/A_G$
LDPE/IFR	2051603	925061	2.18
LDPE/IFR/1%4A	2115391	1088152	1.94

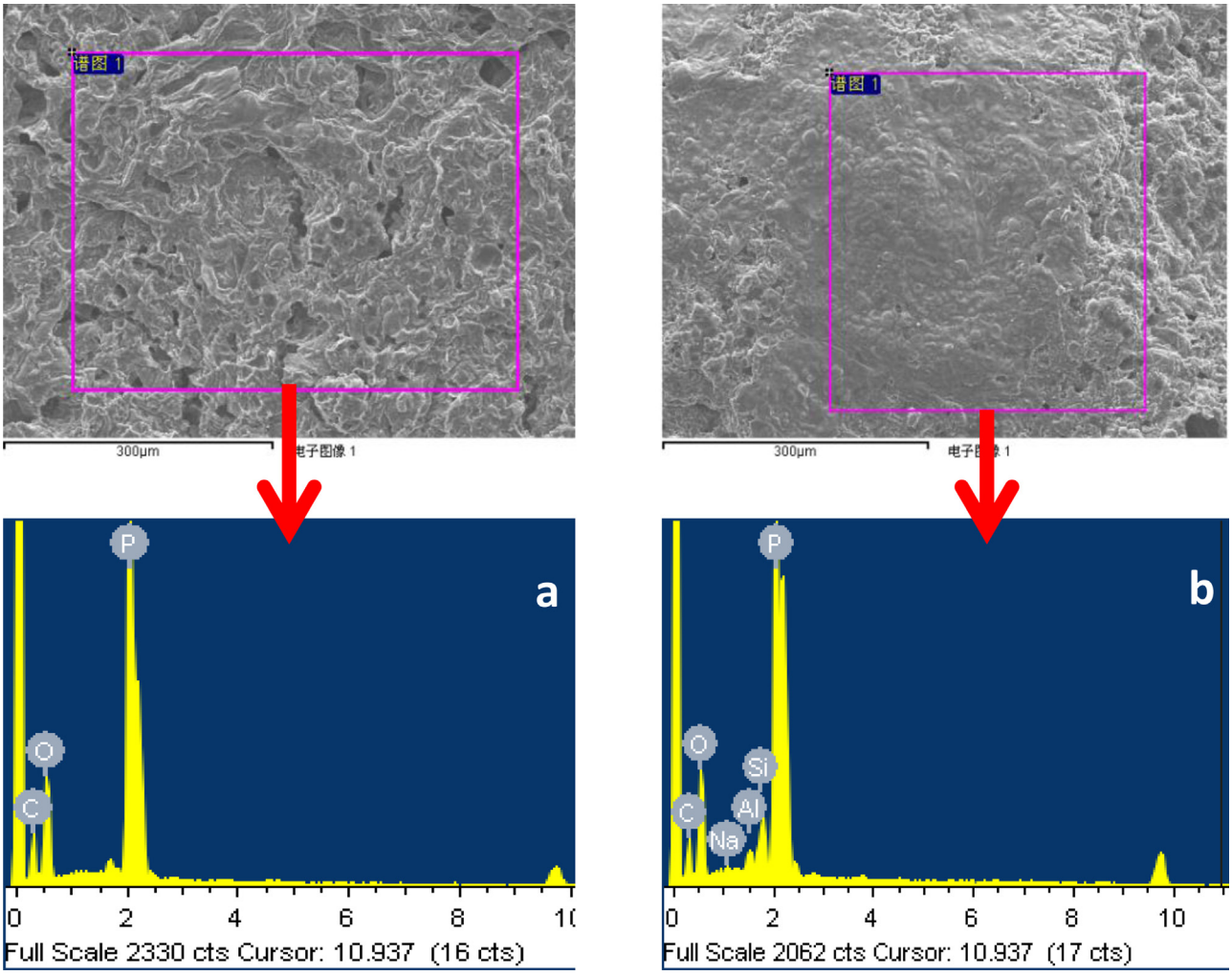

Fig. 13. EDS spectra of char surface (a) LDPE/IFR; (b) LDPE/IFR/1%4A.

Table 6
EDS anslysis results of chars.

Elements	LDPE/IFR		LDPE/IFR/1%4A	
	At%[a]	rc[b]	At%	rc
C K	50.12	–	45.87	–
O K	40.02	0.80	41.69	0.91
P K	9.86	0.20	9.56	0.21
Na K	–	–	0.47	0.01
Al K	–	–	0.74	0.02
Si K	–	–	1.67	0.04

[a] At% means the molar content of elements.
[b] rc means relative molar content of other elements to carbon.

4. Conclusions

Intumescent flame retardant LDPE composites were prepared by melt blending starting from APP, CNCA-DA, and 4A with the LDPE matrix. The introduction of 4A into IFR system based on APP and CNCA-DA presented an obvious synergistic effect in the flame retardant properties of LDPE. A small amount of 4A incorporated into LDPE/IFR played an important role in the improvement of LOI value, and the optimum amount of 4A was 1.0 wt.% according to the LOI, UL-94 and CAT-EFF analysis results. 4A apparently promoted the thermal degradation at advance, especially releasing more NH_3 and the formation of carbonaceous charred layers as revealed by TGA under air atmosphere and TGA/MS analysis. The results of cone calorimeter experiments and digital photos of char residues after CCT tests revealed that there was a synergistic effect between 4A and IFR in LDPE matrix, and the 4A acted as an effective flame retardant synergist and as smoke suppressant. The morphological structure of the char residue proved that the addition of 4A into LDPE/IFR system was benefit to the formation of a compact and homogeneous carbonaceous char layer on the surface of the material during burning, which turned out to be of most importance for the flame retardancy. The studies of LRS and EDS revealed that 4A promoted to form more graphitic structure and remain more P and O in the char layer to increase the interconnected network degree, and thus enhanced the strength of char and improved the flame retardant performance.

Acknowledgments

The financial supports by National Natural Science Foundation of Guangdong China (2014A030310316), Foundation for Distinguished Young Teachers in Higher Education of Guangdong China (YQ2014001) and the National Natural Science Foundation of China (51473185 and 51173214) are gratefully acknowledged.

References

[1] F. Xie, Y.-Z. Wang, B. Yang, Y. Liu, A novel intumescent flame-retardant polyethylene system, Macromol. Mater. Eng. 291 (3) (2006) 247–253.

[2] M. Le Bras, M. Bugajny, J.M. Lefebvre, S. Bourbigot, Use of polyurethanes as char-forming agents in polypropylene intumescent formulations, Polym. Int. 49 (10) (2000) 1115–1124.
[3] D.Y. Wang, Y. Liu, G.X. Ge, Y.Z. Wang, A. Stec, B. Biswas, T.R. Hull, D. Price, Effect of metal chelates on the ignition and early flaming behaviour of intumescent fire-retarded polyethylene systems, Polym. Degrad. Stab. 93 (5) (2008) 1024–1030.
[4] S. Bellayer, E. Tavard, S. Duquesne, A. Piechaczyk, S. Bourbigot, Mechanism of intumescence of a polyethylene/calcium carbonate/stearic acid system, Polym. Degrad. Stab. 94 (5) (2009) 797–803.
[5] S. Bourbigot, M. Le Bras, Carbonization mechanisms resulting from intumescence - part II: association with an ethylene terpolymer and the ammonium polyphosphate-pentaerythritol fire retardant system, Carbon 33 (3) (1995) 283–294.
[6] S.H. Chiu, W.K. Wang, Dynamic flame retardancy of polypropylene filled with ammonium polyphosphate, pentaerythritol and melamine additives, Polymer 39 (10) (1998) 1951–1955.
[7] G. Camino, L. Costa, L. Trossarelli, Study of the mechanism of intumescence in fire retardant polymers: part VI mechanism of ester formation in ammonium polyphosphate-pentaerythritol mixtures, Polym. Degrad. Stab. 12 (3) (1985) 213–218.
[8] A. Riva, G. Camino, L. Fomperie, P. Amigouet, Fire retardant mechanism in intumescent ethylene vinyl acetate compositions, Polym. Degrad. Stab. 82 (2) (2003) 341–346.
[9] G. Camino, L. Costa, L. Trossarelli, Study of the mechanism of intumescence in fire retardant polymers: part I thermal degradation of ammonium polyphosphate/pentaerythritol mixtures, Polym. Degrad. Stab. 6 (4) (1984) 243–252.
[10] G. Camino, L. Costa, L. Trossarelli, Study of the mechanism of intumescence in fire retardant polymers: Part V Mechanism of formation of gaseous products in the thermal degradation of ammonium polyphosphate, Polym. Degrad. Stab. 12 (3) (1985) 203–211.
[11] G. Camino, G. Martinasso, L. Costa, Thermal degradation of pentaerythritol diphosphate, model compound for fire retardant intumescent systems: part I overall thermal degradation, Polym. Degrad. Stab. 27 (3) (1990) 285–296.
[12] X.P. Hu, W.Y. Li, Y.Z. Wang, Synthesis and characterization of a novel nitrogen-containing flame retardant, J. Appl. Polym. Sci. 94 (4) (2004) 1556–1561.
[13] C.M. Feng, Y. Zhang, S.W. Liu, Z.G. Chi, J.R. Xu, Synthesis of novel triazine charring agent and its effect in intumescent flame-retardant polypropylene, J. Appl. Polym. Sci. 123 (6) (2012) 3208–3216.
[14] J.F. Dai, B. Li, Synthesis thermal degradation, and flame retardance of novel triazine ring-containing macromolecules for intumescent flame retardant polypropylene, J. Appl. Polym. Sci. 116 (4) (2010) 2157–2165.
[15] C.M. Feng, Z.W. Li, M.Y. Liang, J.G. Huang, H.B. Liu, Preparation and characterization of a novel oligomeric charring agent and its application in halogen-free flame retardant polypropylene, J. Anal. Appl. Pyrolysis 111 (2015) 238–246.
[16] C.M. Feng, Y. Zhang, S.W. Liu, Z.G. Chi, J.R. Xu, Flame retardancy and thermal degradation behaviors of polypropylene composites with novel intumescent flame retardant and manganese dioxide, J. Anal. Appl. Pyrolysis 104 (2013) 59–67.
[17] C.M. Feng, Y. Zhang, S.W. Liu, Z.G. Chi, J.R. Xu, Synergistic effect of La_2O_3 on the flame retardant properties and the degradation mechanism of a novel PP/IFR system, Polym. Degrad. Stab. 97 (5) (2012) 707–714.
[18] Q. Ren, C.Y. Wan, Y. Zhang, J. Li, An investigation into synergistic effects of rare earth oxides on intumescent flame retardancy of polypropylene/poly(octylene-co-ethylene) blends, Polym. Adv. Technol. 22 (10) (2009) 1414–1421.
[19] X.P. Hu, Y.L. Li, Y.Z. Wang, Synergistic effect of the charring agent on the thermal and flame retardant properties of polyethylene, Macromol. Mater. Eng. 289 (2) (2004) 208–212.
[20] S.B. Nie, Y. Hu, L. Song, et al., Synergistic effect between a char forming agent (CFA) and microencapsulated ammonium polyphosphate on the thermal and flame retardant properties of polypropylene, Polym. Adv. Technol. 19 (8) (2008) 1077–1083.
[21] D. Enescu, A. Frache, M. Lavaselli, O. Monticelli, F. Marino, Novel phosphorous nitrogen intumescent flame retardant system: its effects on flame retardancy and thermal properties of polypropylene, Polym. Degrad. Stab. 98 (1) (2013) 297–305.
[22] M. Dogan, A. Yilmaz, E. Bayramli, Synergistic effect of boron containing substances on flame retardancy and thermal stability of intumescent polypropylene composites, Polym. Degrad. Stab. 95 (12) (2010) 2584–2588.
[23] X.C. Chen, Y.P. Ding, T. Tang, Synergistic effect of nickel formate on the thermal and flame-retardant properties of polypropylene, Polym. Int. 54 (6) (2005) 904–908.
[24] C.M. Feng, Y. Zhang, S.W. Liu, Z.G. Chi, J.R. Xu, Synergistic effects of 4A zeolite on the flame retardant properties and thermal stability of a novel halogen-free PP/IFR composite, Polym. Adv. Technol. 24 (5) (2013) 478–486.
[25] J. Feng, J. Hao, J. Du, R. Yang, Using TGA/FTIR TGA/MS and cone calorimetry to understand thermal degradation and flame retardancy mechanism of poly-carbonate filled with solid bisphenol A bis(diphenyl phosphate) and mont-morillonite, Polym. Degrad. Stab. 97 (4) (2012) 605–614.
[26] X.L. Wang, R. Rathore, P. Songtipya, M.D.M. Jimenez-Gasco, E. Manias, C.A. Wilkie, EVA-layered double hydroxide (nano) composites: mechanism of fire retardancy, Polym. Degrad. Stab. 96 (3) (2011) 301–313.
[27] C.M. Feng, Y. Zhang, D. Liang, S.W. Liu, Z.G. Chi, J.R. Xu, Influence of zinc borate on the flame retardancy and thermal stability of intumescent flame retardant polypropylene composites, J. Anal. Appl. Pyrolysis 115 (2015) 224–232.
[28] F. Tuinstra, J.L. Koenig, Raman spectrum of graphite, J. Chem. Phys. 53 (3) (1970) 1126–1130.